Engineering Science and Technology, an International Journal 22 (2019) 947–955

HOSTED BY

Contents lists available at ScienceDirect

Engineering Science and Technology, an International Journal

journal homepage: www.elsevier.com/locate/jestch

Full Length Article

An internal combustion alternator with both free piston and cylinder

V. Shmelev

Combustion Lab, ICP RAS, Kosygin Str. 4, Moscow 119991, Russia

ARTICLE INFO

Article history:
Received 22 May 2018
Revised 6 December 2018
Accepted 18 January 2019
Available online 31 January 2019

Keywords:
ICE
Alternator
Free piston
Hybrid engines

ABSTRACT

The free-piston generator has more merits than the traditional reciprocating engines, and has been under extensive investigation. This study focuses on the development two novel perspective ideas unlike already advanced the linear free piston generator. These are: (1) to make both piston and cylinder free that provides ideally balancing of the system; (2) to turn from the linear scheme of a generator to rotary design because of simplicity and compactness. The mathematical simulation of operation of the linear two-stroke cycle alternator with both free piston and cylinder was conducted with using the model of zero-dimensional dynamics. Combustion of methane-air mixture with excess air ratio of 1.2 was considered. Both heat and friction losses were taken into account. Operation particularities of such system were analyzed. It was found that oscillation amplitude of moving parts did not exceed of 70 mm at frequency of ~50 Hz for alternator with following basic parameters: cylinder bore of 80 mm, length of 400 mm, piston length of 120 mm. Mass of both piston and cylinder was chosen identical and equal of 3 kg. It was shown that the efficiency of the chemical energy conversion reached of 46%, and specific power was high as 40 kW/l at compression ratio of 40. The lab scale pneumatic alternator in rotor variant with both free rotor and cylindrical body was assembled for experimental demonstration of rotary design capability. The alternator was fed with compressed air of low pressure below of 6 atm. The electrical power in the load reached of 10 W at input power with intake compressed air about 100 W. The results indicate that alternators with both free piston and cylinder in linear and rotary designs have the potential to achieve high efficiency and provide the vibration – free operation.

1. Introduction

Nowadays, there is an acute problem of development of mobile autonomous mini-power stations and electrical generators of a new generation. Different mobile autonomous mini-power stations used now consist of two bound together technical units providing conversion of the organic fuel energy to the electric power. The first unit is a piston internal combustion engine (ICE). The second unit is rotating electrical generator. In recent years, the electrical generator of new type as a mono energy block was designed on the base of linear internal combustion engine with a free piston [1–12]. This generator consists of a free piston engine (FPE) coupled to a linear electric machine. Simple design of the electrical machinery makes this an interesting concept. The general working principle is that the high-temperature and high-pressure gas after the heat release process in the cylinder drives the piston assembly to reciprocate, and the generator converts parts of the mechanical energy into electricity. Such FPE generator has promising advantages. The "crankless" configuration allows the novel engine to operate with variable stroke length and compression ratio, which gives extensive performance advantages, such as multi-fuel possibilities, lower friction losses from fewer motion parts, high power density, fast transient response and combustion optimization flexibility.

This technology is currently being explored by a number of research groups worldwide [11–26]. Most researchers generally applied zero-dimensional empirical models (such as Wiebe model) [11–19] to model the combustion process of free-piston engine generator in the linear design. They simulated the gas motion and heat release of combustion process with simplified functions, ignored or weakened the influence of gas motion and species distribution. The zero-dimensional model approach is enough effective and allows revealing a control strategy to improve the output power for a free-piston linear generator. The results of study [27] stated that the proposed control strategy can improve the output power by around 7–10% with the same fuel cycle mass. Validation between numerical modeling of the spark-ignited free-piston linear generator and its prototype showed a good fitting. The efficiency of 31.5% at a power output of 4 kW was reached [12].

Single and multi-zone Chemkin model with detailed chemical kinetics, and unique piston dynamics extracted from one dimen-

E-mail address: shmelev.05@mail.ru.

Peer review under responsibility of Karabuk University.

https://doi.org/10.1016/j.jestch.2019.01.009
2215-0986/

Nomenclature

Symbols

E	specific internal energy of gas, J/kg
E_d	energy of water dissociation, J/mols
F_f	friction force, N
F_e	electromagnetic interaction force, N
H	specific enthalpy, J/kg
K_{eq}	equilibrium constant, atm$^{-0.5}$
k_e	parameter of an electrical load
q	gas flow rate, kg/m^2•s
M_k	mass of piston or cylinder, kg
m	mass of gas, kg
m_m	mass of fuel, kg
N_w	number of water vapor, mol
n	polytropic exponent
P	pressure, Pa
P_{in}	intake pressure, Pa
S	cross-section of the cylinder, m^2
t	running time, s
V_a	alternator volume, m^3
V_i	volume, m^3
U_i	speed of piston or cylinder, m/s
w_i	consumption rate of methane, kg/s
W_c	heat release, W
W_h	heat losses, W
W_e	electrical power, W

Greek letters

α	degree of dissociation
ξ_m	current mole fractions of methane in mixture
ξ_{ox}	current mole fractions of oxygen in mixture
η_c	intake parameter
τ_c	characteristic turbulent combustion time, s
τ_{ig}	characteristic ignition delay time, s

Abbreviations

ICE	internal combustion engine
FPE	free piston engine
CFD	computational fluid dynamics
EMF	electromotive force
ICA	internal combustion alternator

sional gas dynamic model, have been used to analyze the combustion characteristics and engine performance [20]. A dynamic model of the complete free piston engine has been used to predict the piston motion, while the commercial 1-D code BOOST has been used to simulate the gas exchange [21]. Combustion has been simulated by detailed chemistry calculations in SENKIN. The results show that the piston motion of the FPE differs substantially from the piston motion in a conventional internal combustion engine. It was found that the efficiency of the FPE depended on two effects, namely high compression and fast combustion.

Some researchers calculated the combustion performances of a free-piston engine generator using computational fluid dynamics (CFD) software to define its combustion efficiency [14,22–26]. They focused on a numerical simulation for the research on the combustion process of a free-piston diesel engine generator by adopting coupled models of zero-dimensional dynamics and multi-dimensional CFD combustion, the simulation was validated with tested data from a running free-piston engine generator prototype.

However, in spite of numerous advantages of a free piston linear generator there are some issues. FPE linear generator is still hindered with problems such as misfire, unstable operation, piston motion control challenges and complexity in the control system design [7–10]. There is danger of collisions between the piston and the cylinder head in the single piston design or collision between both pistons in the two piston design. The FPE linear generator with single free piston and two end combustion chambers is not balanced in principle; therefore, operation of such generator runs with strong vibrations if there is not a massive bed. The linear generator with two free pistons moving in opposite directions and single central combustion chamber theoretically can be balanced. However, such design requires a complicated electronic control system for motion correction of the pistons.

The ICE design with free piston without any indicated disadvantages was suggested in [28,29]. Here, not only the piston but also the cylinder is free. Such engine is the absolutely balanced machine because the center of mass of the system is immobile at interaction of both moving parts (Fig. 1). It essentially simplifies the control system. The possible design of the linear generator on the base of a two - strokes ICE using a new principle is displayed in Fig. 2. The ring-type magnets are fixed on the piston and the electrical winding with the magnetic conductor is located on the cylinder (Fig. 2a). In this system, there is no problem of bumping a free piston against the cylinder head at high compression ratio at misfiring because of a free cylinder. The severe problem of the electronic control on fuel supply disappears also. Basically, the scheme of an ideal balanced linear alternator is realized where the motion of both "armature" and "stator" is caused by a direct action of the pressure under combustion of the air-fuel mixture. Changing the magnetic flux occurs at mutual displacements of both free piston and cylinder, and the EMF is induced in the electrical winding. Note that in the considered system, the relative piston magnets velocity concerning the electrical winding of the cylinder is higher than in the scheme with the fixed cylinder. Basically, that is an idea of the new type FPE alternator which can be named shortly as internal combustion alternator (ICA), analogically to ICE.

The simpler scheme of ICA with external magnets is presented in Fig. 2b. The light magnetic conductor is located on the cylinder. Here, the external electro magnetic system is immobile and can be connected with the bed. The vibration level is dropped due to reduced essentially mass of both free piston and cylinder. It is necessary to connect the free piston with the electro magnetic system for absolute excluding any vibrations. This is difficult to do structurally in the linear alternator scheme; however, it can be easily solved in the rotary design.

Design of a compact closed two-stroke rotary alternator with the piston – rotor is very attractive (Fig. 3). The rotor is connected with a ring-type electro magnetic system which is located on a circumference of the free body. Supplying fresh mixture and exhaust of combustion products can be made through a hollow shaft with window type valves. The theory of the rotary engine with a free rotor was considered in Ref. [29].

The purpose of this study is to introduce two novel perspective ideas unlike already advanced the linear free piston generator: to make both the piston and cylinder free that provides ideally balancing of the system; to test the generator of rotary design. In the first case the mathematical simulation of operation of the linear internal combustion alternator with both free piston and cylinder was done. The operation features of such system were analyzed. In the second case the experimental lab scale model of pneumonic alternator in rotary design was demonstrated.

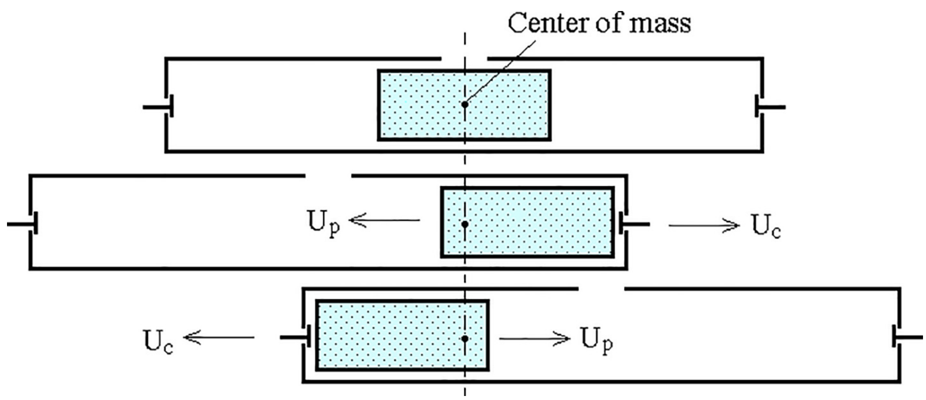

Fig. 1. Motion of both free piston and cylinder.

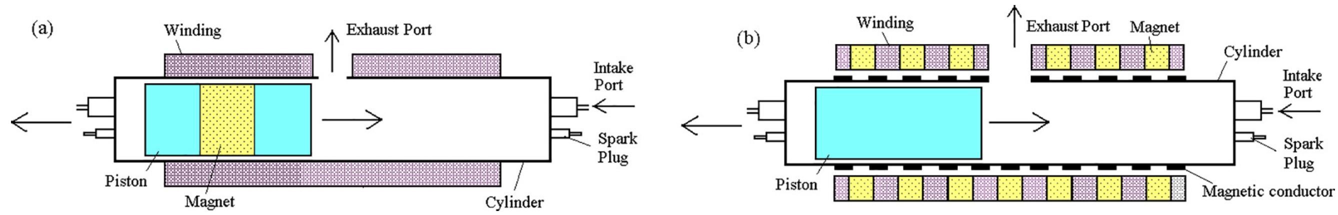

Fig. 2. Cross-sectional view of linear ICA with internal (a) and external magnets (b).

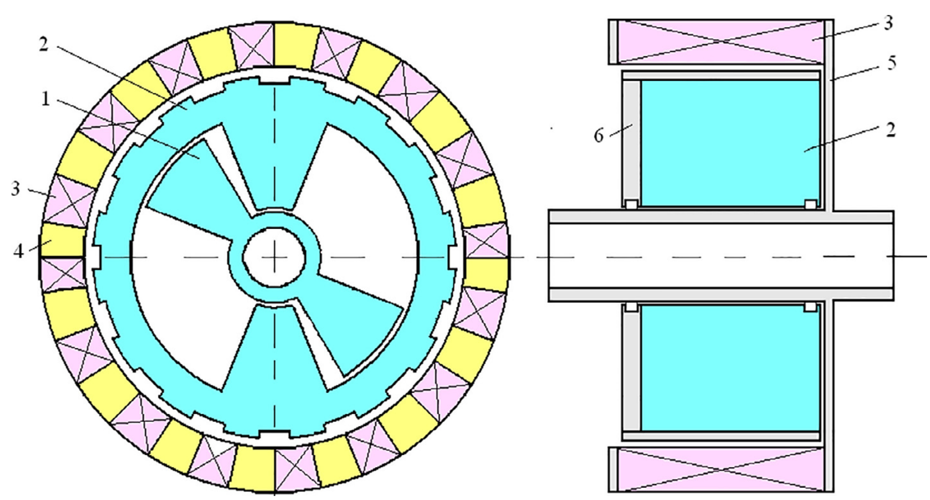

Fig. 3. Cross-sectional view of rotor ICA with both free rotor and body: 1 – free rotor, 2 – free body with the magnetic conductor, 3 – electro winding, 4 – magnets, 5 – connection of the rotor with electromagnets, 6 – cover.

2. Mathematical model

The simple 0-D simulation model was used for describing operation of the linear ICA with both free piston and cylinder. It was supposed, that ICA was fed with methane–air mixture, and the free piston moved inside the free cylinder, executing reciprocating motion. Gas mixture was compressed alternately in the end chambers of the cylinder. The intake ports are located in the cylinder heads, and the exhaust port is located in the central part of the cylinder. All ports are equipped with valves of the conforming operation. Both piston and cylinder replace in opposite directions so that a center of mass of the system is immobile.

The two-stroke operation cycle is realized. It is supposed that the exhaust valve is opened at the end of the power stroke. Simultaneously the intake valve is opened and air-fuel mixture enters into the cylinder under some pressure, and blowdown occurs. This incoming mixture pushes much remaining exhaust gases out through the open exhaust valve, and the cylinder is filled with combustible air-fuel mixture in the scavenging process. All valves are closed after scavenging. The compressed mixture is ignited by spark plug at the end of the compression stroke. Combustion energy is converted to electrical energy in the power stroke. Without any detail consideration of the electromagnetic alternator system, it is assumed that the electrical power in a load defined by the electromagnetic interaction force is in the square dependence from the relative velocity of both piston and cylinder.

The follow equations describes change of the internal energy, gas mass and replacements of both piston and cylinder taking into account the heat release at combustion of the methane-air mixture, heat and friction losses and useful work [30–34]:

$$
\begin{aligned}
&\frac{dE_i m_i}{dt} = P_i \frac{dV_i}{dt} + H_i^+ q_i^+ - H_i^- q_i^- + W_{ci} - W_{hi}\\
&\frac{dm_i}{dt} = q_i^+ - q_i^-\\
&\frac{dm_{mi}}{dt} = -w_i + \xi_{m0} q_i^+\\
&\frac{dV_i}{dt} = SU(t)\\
&M_k \frac{dU_k}{dt} = S(P_2 - P_1) - F_f - F_e
\end{aligned}
\tag{1}
$$

Here, i = 1, 2 – subscript defining the cylinder chamber; k = 1, 2 – defines the piston and cylinder respectively; "0" – initial values; superscripts "+" and "−" mark of intake and exhaust gas respectively. Expression for flow rate was taken from [34]. Usually in ICE theory, Wiebe function converted to time used for description of the combustion process [30]. The similar empirical approach for function W_c was adopted here. It was supposed that after ignition in TDC, the mixture was burned out during of the characteristic combustion time τ_c. The process of chemical conversion of the mixture can be interpreted as turbulent combustion. Accordingly, the mass consumption rate of methane was expressed as $w_i = \frac{dm_{mi}}{dt} = \frac{m_{mi}}{\tau_c}$. Dissociation of combustion products was accounted as correction ΔE to specific combustion energy. The value $\Delta E = E_d N_w \alpha$ can be expressed through degree of water vapor decomposition in the reaction:

$H_2O \rightarrow H_2 + 0.5O_2$.

Here E_d = 241.84 kJ/mol. The degree of water vapor dissociation is expressed through the equilibrium constant as $\alpha = \left(\frac{0.71}{K_{eq}P^{1/2}}\right)^{2/3}$. The temperature dependences of specific heat capacity for intake mixture and combustion product were taken from Ref. [35]. The heat losses rate was based on the Woschni model [30,31]. Expression for the friction force between the piston and cylinder was taken from Ref. [31]. The electrical power in a load was calculated as $W_e = \frac{k_e}{t}\int_0^t U_m^2 dt$, where $U_m = |U_1 - U_2|$. The system (1) was supplemented with a perfect gas law.

Initial conditions for the central piston position in the cylinder at t = 0: $U_1 = U_0$, $U_2 = -U_0 M_1/M_2$, P_0 = 1 atm, T_0 = 300 K, m_m = 0. The initial velocity U_0 was set equal of 14 m/s. The combustion time of the mixture is determined by turbulent combustion speed U_{tc} and, therefore, depends from gas dynamics of the cylinder filling. It is typically U_{tc} = 10–40 m/s for ICE. The characteristic time $\tau_c = 410^{-4}$ s was chosen, so the turbulent combustion speed should be of 25 m/s for the characteristic combustion zone of ~10 mm. Choosing greater value τ_c result in uncompleted combustion of methane.

3. Results and discussion

Obviously, that the operation regime of the alternator essentially depends on many input parameters, such as length and mass of both piston and cylinder, time of valves opening, ignition delay, cylinder scavenging, electrical load, etc. Thus, the optimization of solution is very complicated multi parameter problem. The simulation was conducted for some concrete input parameters of the problem that gave the insight about an operation peculiarity of such system. Calculations were carried out for the ICA variant with internal location of magnets (Fig. 2a) at following parameters: the cylinder bore of 80 mm, length of 400 mm, piston length of 120 mm, reduced diameter of the exhaust valve of 50 mm, intake valve diameter of 20 mm. Intake pressure of the methane-air mixture was varied from 1 up to 4 atm. The excess air ratio was equal of 1.2.

Mass of both piston and cylinder was chosen identical and equal of 3 kg. It was assumed that the exhaust of the combustion products and filling the cylinder with fresh mixture occurred simultaneously during the compression stroke. Operation of both exhaust and intake valves was synchronous. The opening time of the valves corresponded with beginning the compression stroke. The closing time of the valves was chosen by varied intake parameter η_c which determined the start of real compression process at volume $\eta_c V_a$. The intake pressure was selected so that to provide practically of 100% scavenging of the cylinder with the fresh mixture, i.e. the intake gas mass was equal to running gas mass in cylinder. During replacement of the piston from BDC to TDC the mass of methane increased quickly, reached the constant value and then fell dramatically to zero after ignition and combustion in beginning of the power stroke.

Dependences $P(\bar{V})$ and $T(\bar{V})$ are presented by P-V and T-V diagrams respectively in Fig. 4. Here, $\bar{V} = V/V_0$ is dimensionless displacement volume. It was considered two cases for adjusted parameters η_c, k_e and P_{in}. The alternator performance reached the maximum value at selected parameters. It can be seen from figures that the less parameter η_c the lower compression pressures and the more compression temperature. It is explained by that the smaller mass of gas mixture is required for cylinder scavenging in the first case.

The dimensionless mass of the gas mixture $Z = m/m_0$ increases approximately in 1.6 times from value of 0.26 up to 0.423 under the intake pressure growth from 1.3 up to 4.17 atm at increasing the parameter η_c from 0.6 up to 0.8 (Fig. 5). Here m_0 – mass of

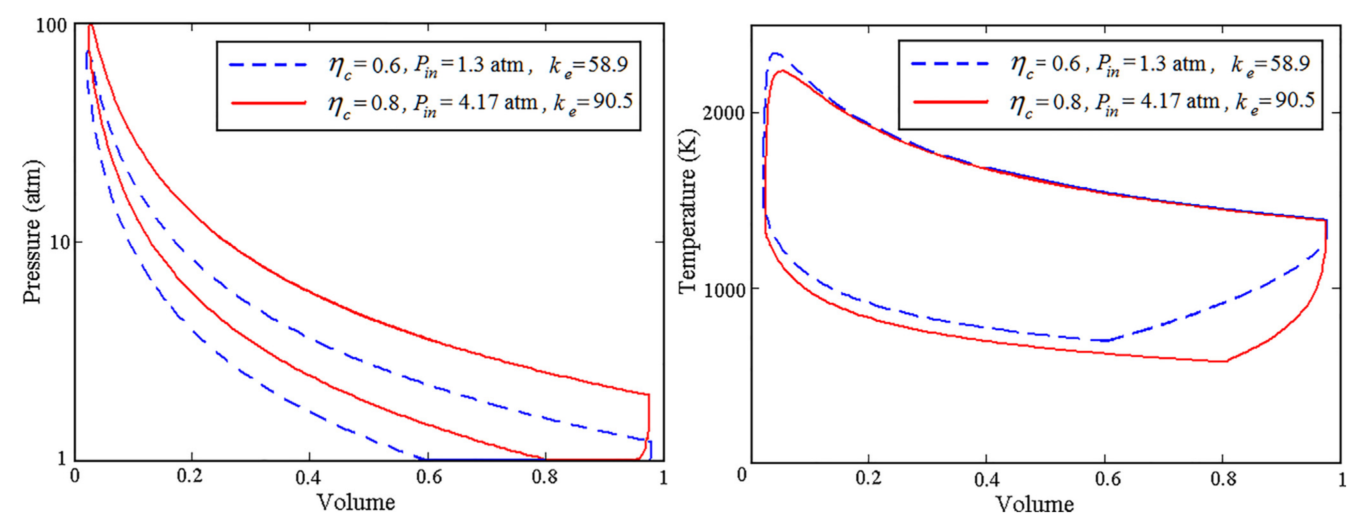

Fig. 4. P-V and T-V diagrams at compression ratio of 40.

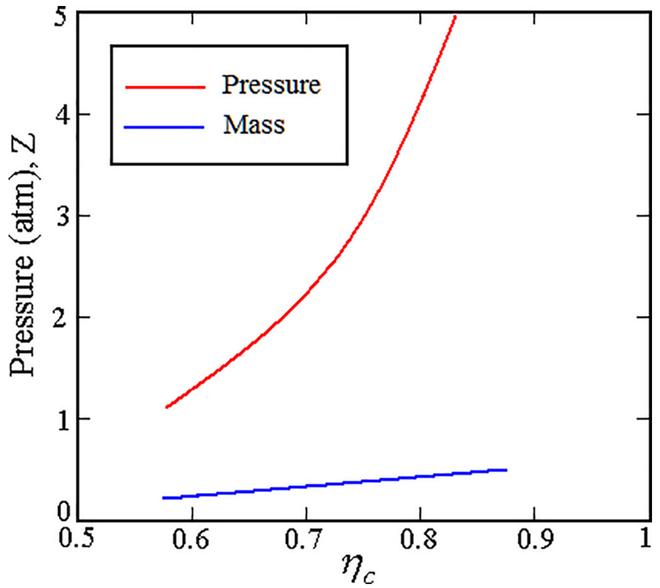

Fig. 5. Dependence of intake pressure and dimensionless mass of the mixture in the cylinder on the intake parameter.

air in the cylinder at initial conditions P_0 and T_0. Note, the function $P_{in}(\eta_c)$ grows faster than function $Z(\eta_c)$ with increasing of the parameter η_c because the speed of both piston and cylinder increases with growing mass of the combustible mixture and, therefore, intake time of fresh mixture is reduced.

The dimensionless values of the piston (cylinder) speed $\bar{U} = \frac{U}{U_0}$ and mass of combustible $\bar{m}_m = \frac{m_m}{m_0}$ for selected parameters η_c, k_e and P_{in} submitted in Fig. 6. The right part of the loop function $\bar{m}_m = f(\bar{V})$ corresponds to continuous feeding the combustible into the cylinder; the left part of the closed loop is determined by its burning. As concerning the dependence of the piston (cylinder) speed on the volume $\bar{U} = f(\bar{V})$, it is strong flat and far from a sinusoidal view. It is explained by strong deceleration of both piston and cylinder by the electromagnetic interaction force.

Changes of both the maximum pressure and temperature from the compression ratio at variable parameters η_c are submitted in Fig. 7. The maximum pressure increases proportionally to the growth of the compression ratio, while the maximum temperature smoothly decreases. The temperature drop is connected with required increasing input gas mass. The maximum pressure

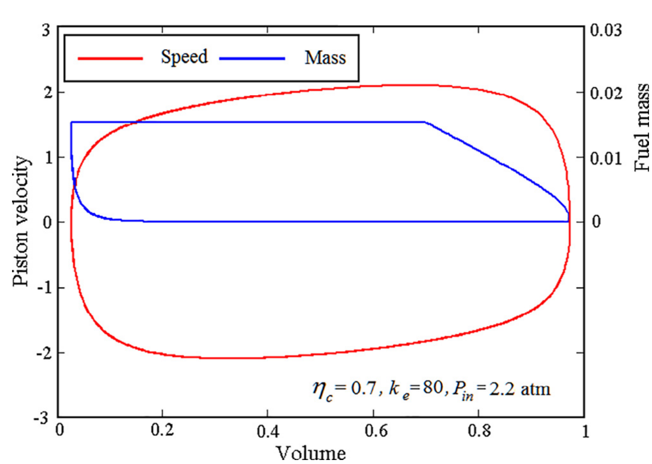

Fig. 6. Dependence of the piston speed and mass of combustible on the displacement volume.

increases from 20 up to 130 atm and maximum temperature a little bit decreases from 2500 up to 2200 K within the compression ratio range from 10 up to 80 and k_e from 75 up to 56 for optimum regime of the alternator operation at η_c = 0.6 (Fig. 7a). Increase of the parameter η_c up to 0.8 results in increasing the maximum pressure and small drop of the temperature (Fig. 7b). The growth of the maximum pressure is connected with required increasing input gas mass to provide the optimum operation regime of the alternator. Accordingly to adjusted value P_{in} (Fig. 5), the coefficient k_e has to be changed from 110 up to 80 within the compression ratio range from 10 up to 80.

The frequency of the process is within the range of 40–50 Hz (Fig. 8) at moderate compression ratio 40–60, that is optimum for alternating electric current generators, and an oscillation amplitude of both piston and cylinder is almost constant ~63–68 mm within the wide range of the compression ratio. Obviously, the operation frequency will be change with changing the weight of moving parts of the alternator.

The efficiency of the chemical energy conversion to the electrical energy has a weakly expressed maximum (near 41%) at η_c = 0.6 around of the compression ratio ~90 and k_e = 90 (Fig. 9a). The maximum electrical efficiency grows and shifts in area of high compression with increasing of the parameter η_c. It is connected with increasing mass of the intake mixture (Fig. 5). Small drop of the electrical efficiency at high compression ratios is connected with increasing the heat losses. The maximum performance is high as 46% for η_c = 0.8, and it reaches this value at the compression ratio closed to 82 at k_e = 80 (Fig. 9b).

The specific electrical power of the alternator increases with increasing of both compression ratio and parameter η_c (Fig. 9). The great value of 58 kW/l is reached at the compression ratio ~80 at η_c = 0.8. Note that the specific mechanical power is high as ~20 kW/l for conventional two-stroke gasoline ICE. Simultaneous growth of both the specific electrical power and oscillation frequency provides the almost constant oscillation amplitude (Fig. 8) because the oscillation amplitude is proportional to $\sqrt{W_e}$ and inversely proportional to oscillation frequency accordantly to the expression for W_e.

Obviously, that the spontaneous self ignition of the methane-air mixture by compression ahead of the combustion front is possible at the great compression ratio. It is necessary to compare both characteristic times of ignition delay τ_{ig} and turbulent combustion time τ_c for estimation of the critical condition of self ignition of the mixture. The value τ_{ig} for methane–air mixture can be calculated from the expression [36]:

$$\tau_{ig} = \xi_m^{0.3}\xi_{ox}^{-1}P^{-0.7}\left[2.510^{10}\exp(-25{,}000/T) + 2.510^{4}\exp(-10{,}000/T)\right]^{-1}$$

Dependences of the combustion temperature T_c after forced ignition of the mixture and the fresh mixture temperature T_f ahead of flame front on the pressure are submitted in Fig. 10. Heating the fresh mixture by compression is described satisfactorily by the polytropic ratio $T/T_0 = (P/P_0)^{\frac{n-1}{n}}$ with the polytropic exponent n = 1.235 (curve 2). It can be seen that the times relation $\bar{\tau} = \tau_{ig}/\tau_c > 1$, though it is close to unit at the maximum process pressure. It means that self ignition mode is not realized at compression ratios less than 28. The self ignition of the mixture ahead of the flame front is possible during of compression and burning at final compression ratio above 28. This case is equivalent of reduction of the characteristic burning time τ_c, that results in some increasing the maximum pressure. Such output parameters of the process, as the temperature, frequency and oscillation amplitude, efficiency of the chemical energy conversion to electrical one are varied insignificantly (less, than 10%) at reduction of τ_c in four times.

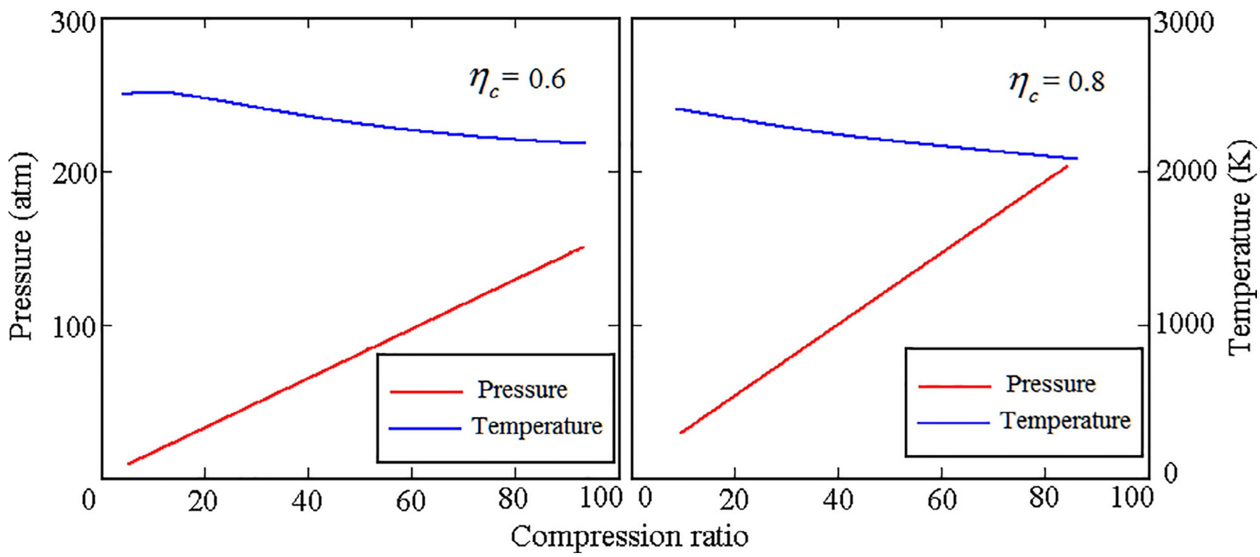

Fig. 7. Dependence of the maximum pressure and combustion temperature on the compression ratio.

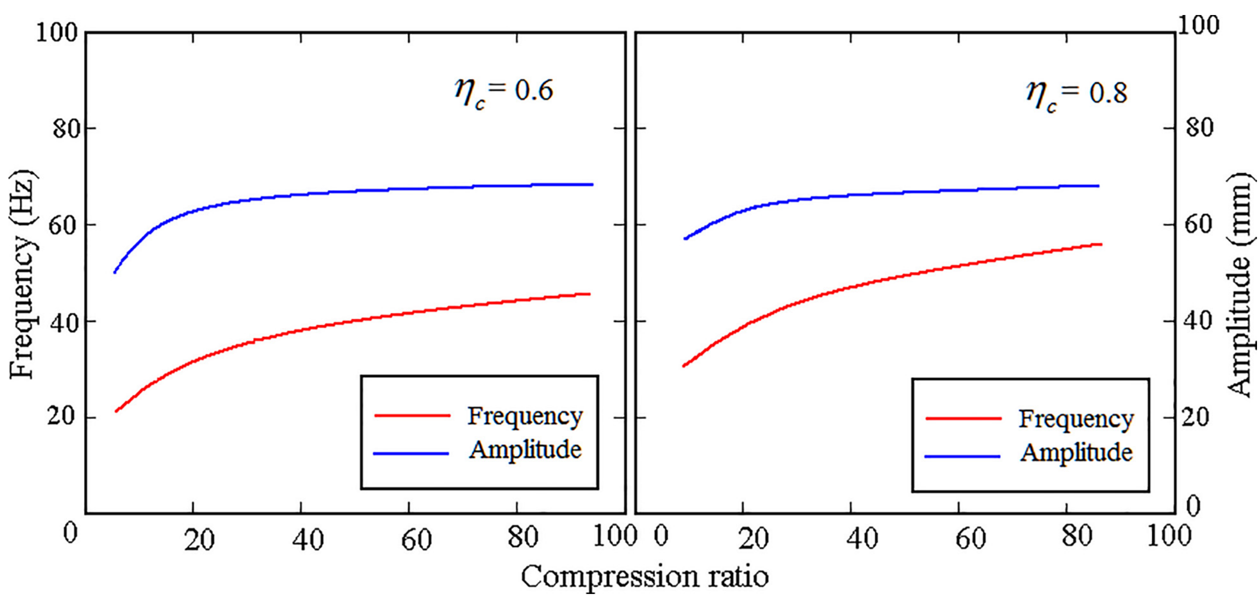

Fig. 8. Dependence of the frequency and oscillation amplitude of both piston and cylinder on the compression ratio.

Thus, the conducted simulation demonstrated a high power efficiency of the given type ICA. Apparently, that optimization of the process will allow increasing even more the specific power and the power performance of the alternator.

4. Preliminary experiments

Results of an experimental investigation of the free piston pneumatic expander-linear generator were presented in Ref. [37]. The test rig using compressed air as working fluid was established. The motion characteristics, dynamic characteristics and the indicated efficiency of the pneumatic linear generator were analyzed. The maximum power output of 19 W was achieved when the intake pressure was 2.0 bar and the operation frequency was 2.5 Hz.

In our study the lab scale pneumatic alternator in rotary design with both free rotor and cylindrical body was assembled for experimental demonstration of ICA capability (Fig. 11). Such design surpasses essentially in the assembling simplicity of own engine and electrical generator in opposite to the linear variant, taking into account the magnets location outside of the cylinder space. The simplified design with the one-sector rotor was chose in comparison with the scheme in Fig. 3. The single body sector was installed inside the cylindrical body and fixed with it. The exhaust port in the body was located opposite this sector. Intake of compressed air occurred through the electromagnetic valves mounted from both sides of the body sector. A conventional three-phase 60 W electrical generator 4T139QMB of SCOOTER-M Ltd was connected with the assembly. The rotor with magnets of the electrical generator was fixed with the assembly rotor, and the stator was attached to the assembly body. A 10 W lamp was used as an electrical load. Main specifications of the setup: inner body diameter was 100 mm, cross-section of total rectangular working volume of 0.17 L was 40 mm of width and 30 mm of height, the exhaust port of 10 × 40 mm. Labyrinth seals were used in both rotor and body

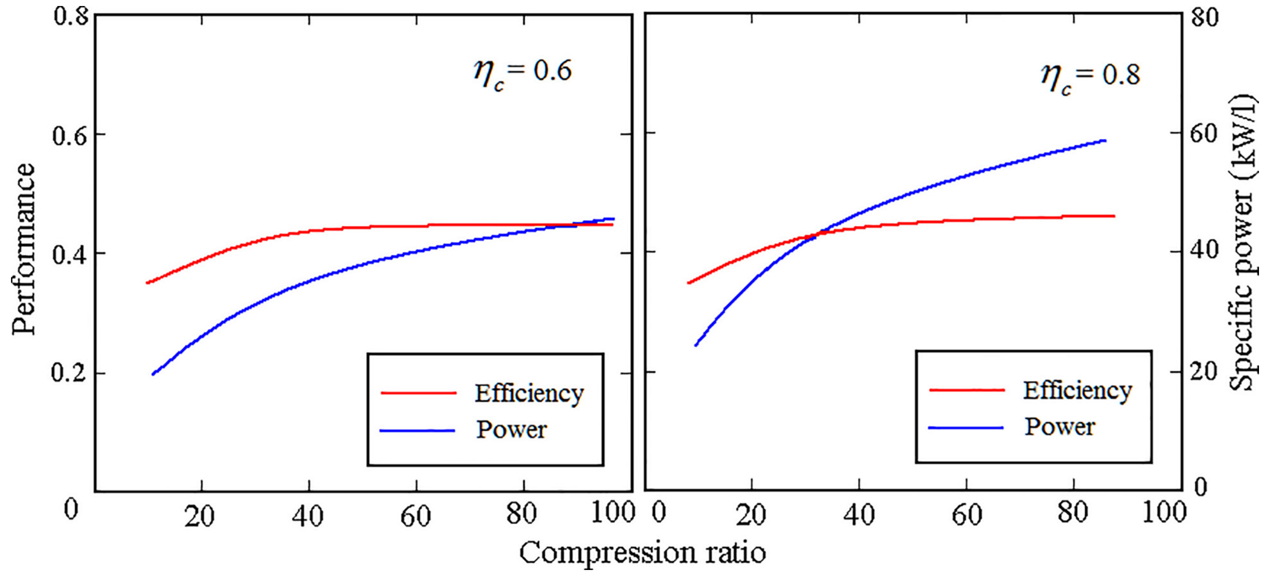

Fig. 9. Dependence of energy conversion efficiency and specific power on the compression ratio.

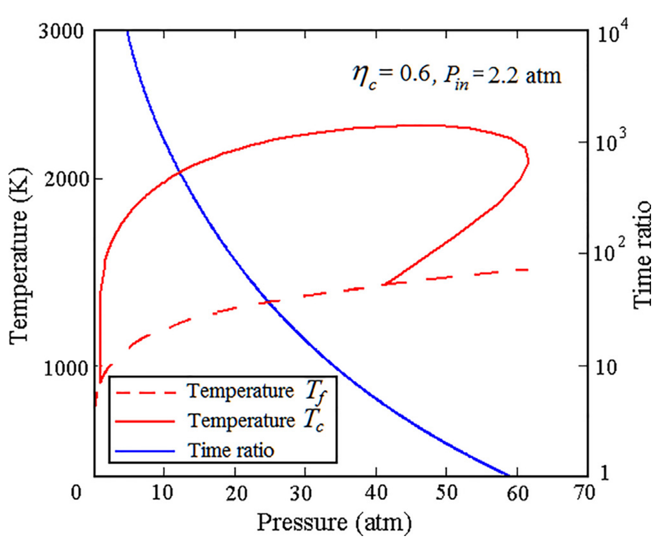

Fig. 10. The temperatures of fresh mixture ahead the combustion front and relation of characteristic times of self ignition and combustion. The final compression ratio is 28.

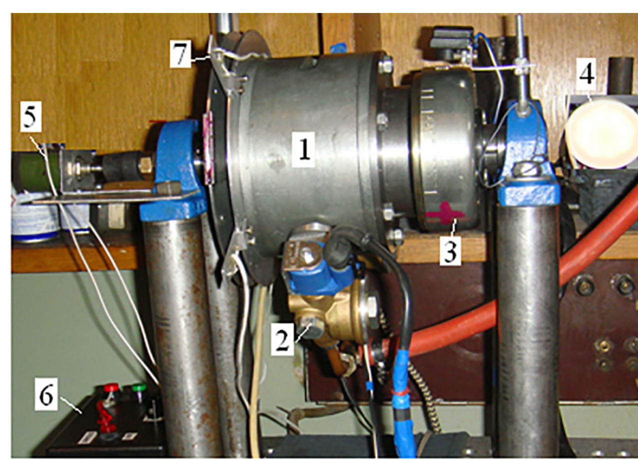

Fig. 11. Image of the rotor pneumatic alternator. 1 – Free body, 2 – electromagnetic valve, 3 – stator of the electric generator, 4 – electrical load, 5 – slewing sensor, 6 – electronic control system, 7 – reed switch.

sectors, however additional compressive sealing vanes could be installed in the sectors. In this case the compression was increased essentially. The automobile electromagnetic valves OMVL BFC of Italy with a flow cross section of 28 mm^2 were used as intake valves for compressed air. The moment and duration of the air injection could be controlled with the electronic controller using reed switches. The slewing sensor for registration of the rotor oscillation amplitude was established from another side of assembly body. Simultaneously, the body oscillation amplitude was fixed by the marker. The small pressure transducer 24PCGFA6D of Honeywell was inserted into the body near the body sector. By estimations, the maximum electrical power of the given alternator can reach approximately 20 kW at combustion of the stoichiometric methane–air mixture providing 50% conversion efficiency of chemical energy to electrical. However, the variant with combustion did not considered in the given study so far. In the preliminary experiments the alternator was fed with compressed air of low pressure below of 6 atm. In this case the compressive vanes were removed because the compression pressure surpassed capabilities of our air compressor.

Results of experiments showed that the alternator operated steady with the oscillation frequency of 5–15 Hz at air supply from 2 up to 6 atm. The compression ratio was low, did not exceed 2, thus the electrical power in the load was ~10 W at input power with intake compressed air near 100 W.

The absolute pressure and rotor oscillation oscillogram as well as voltage signal $U_v = 15$ V from the valve feeding the alternator with compressed air are displayed in Fig. 12. Here, the maximum pressure P was 3.5 atm, maximum rotor oscillation amplitude φ was 30°. Nonmonotonic pressure changing in the compression stroke can be explained by gas escaping because of not enough effective ability of labyrinth seals at low speed of rotor oscillations.

Thereby, the preliminary experiments demonstrated viability of idea of an alternator with both free piston and cylinder in the rotary design.

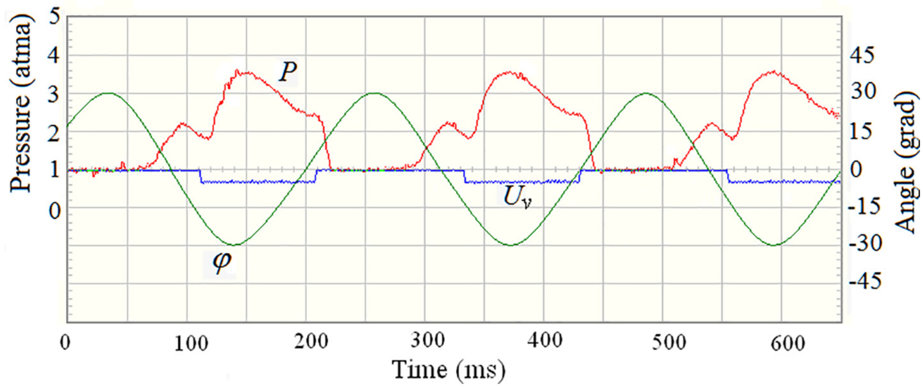

Fig. 12. Oscillogram of the pressure and rotor oscillation amplitude and voltage on the electromagnetic valve.

5. Conclusions

Two novel perspective ideas unlike advanced the linear electrical free piston generator was considered in this study. It was suggested to make both the piston and cylinder free. It provides ideally balancing of the system. Also, it is interesting to turn from the linear scheme of the generator to rotary design. The mathematical simulation of operation of an internal combustion alternator with both free piston and cylinder in linear design was conducted. Variant of the alternator with internal location of magnets was considered. The operation particularities of such system were analyzed for some concrete input parameters of the problem. Operation of the experimental pneumonic lab scale model of the alternator executed in the compact rotary design was demonstrated.

The main conclusions can be summarized as follows:

(1) Calculations were shown that the maximum pressure increased proportionally to the growth of the compression ratio, while the temperature smoothly decreased. Increase of the intake parameter resulted in increasing of the maximum pressure and small drop of the temperature. It is connected with required increasing input gas mass to provide the optimum operation regime of the alternator.
(2) The frequency of the process was within the range of 40–50 Hz and the oscillation amplitude of both piston and cylinder was almost constant ~63–68 mm at moderate compression ratio of 40–60.
(3) The specific electrical power of the alternator grew with increase of both the compression ratio and intake parameter. The maximum electrical efficiency grows and shifts in area of high compression with increasing of the intake parameter. It is connected with increasing mass of the intake mixture. Small drop of the electrical efficiency at high compression ratios is connected with increasing the heat losses. The great specific power reached of ~40–50 kW/l at the compression ratio of 40–60 and intake parameter of 0.8. Conversion efficiency of chemical energy to electrical at combustion of methane–air mixture reached of 46% in not optimized variant.
(4) The experimental rotary alternator of simplified one-sector design was assembled. The alternator was fed with compressed air of low pressure below of 6 atm. Results of preliminary experiments showed that the alternator operated stably with the oscillation frequency of 5–15 Hz at air supply from 2 up to 6 atm. The electrical power in the load reached of 10 W at input power with intake compressed air about 100 W.

This paper focused on developing novel ideas for ICA. Creation of experimental setups on combustion and validation between the numerical and experimental results is planed in our future work, which will be continuation of efforts to reach the maximum performance of novel design ICA.

Acknowledgements

The authors would like to thank the FASO for their attention to this work conducted within the state task for ICP RAS 0082-2014-0012. State registration number is AAAA-A17-117040610346-5.

References

[1] P. Famouri, W.R. Cawthorne, N. Clark, S. Nandkumar, C. Atkinson, R. Atkinson, et al., Design and testing of a novel linear alternator and engine system for remote electrical power generation, in: Proc. IEEE Power Engineering Society Winter Meeting, 1999, pp. 108–112, https://doi.org/10.1109/PESW.1999.747434.
[2] P. Blarigan, Advanced internal combustion electrical generator, in: Proc. 2001 DOE Hydrogen Program Review, NREL/CP-570-30535, 2001, p. 23.
[3] V. Duchanin, A. Kecaris, Design analysis of the reciprocal motion automobile generator, Proc. MAMI 14 (2012) 97–104.
[4] D. Carter, E. Wechener, The Free Piston Power Pack: Sustainable Power for Hybrid Electric Vehicles, SAE Paper, 2003. 2003–01-3277.
[5] O. Vysoky, Linear combustion engine as main energy unit for hybrid vehicles, in: TRANSTEC Prague, 2007, pp. 1–9.
[6] R. Mikalsen, A. Roskilly, A review of free-piston engine history and applications, Appl. Therm. Eng. 27 (2007) 2339–2352.
[7] W. Arshad, A Low-Leakage Linear Transverse-Flux Machine for a Free-Piston Generator, Elektrotekniska System, Stockholm, 2003.
[8] C. Yuan, H. Feng, Y. He, J. Xu, Combustion characteristics analysis of a free-piston engine generator coupling with dynamic and scavenging, Energy 102 (2016) 637–649.
[9] N.B. Hung, O. Lim, A review of free-piston linear engines, Appl. Energy 178 (2016) 78–97.
[10] C. Guo, H. Feng, B. Jia, Z. Zuo, Y. Guo, T. Roskilly, Research on the operation characteristics of a free-piston linear generator: numerical model and experimental results, Energy Convers. Manage, 2016. Doi: https://doi.org/10.1016/j.enconman.2016.11.010.
[11] H. Kosaka, T. Akita, K. Moriya, S. Goto, et al., in: Development of Free Piston Engine Linear Generator System Part 1 – Investigation of Fundamental Characteristics, SAE Technical Paper 2014-01-1203, 2014, https://doi.org/10.4271/2014-01-1203.
[12] B. Jia, Z. Zuo, G. Tian, H. Feng, A. Roskilly, Development and validation of a free-piston engine generator numerical model, Energy Convers. Manage. 91 (2015) 333–341.
[13] J. Kim, C. Bae, G. Kim, Simulation on the effect of the combustion parameters on the piston dynamics and engine performance using the Wiebe function in a free piston engine, Appl. Energy 107 (2013) 446–455.
[14] R. Mikalsen, A. Roskilly, Performance simulation of a spark ignited free-piston engine generator, Appl. Therm. Eng. 28 (2008) 1726–1733.
[15] J. Hu, W. Wu, S. Yuan, C. Jing, Mathematical modeling of a hydraulic free piston engine considering hydraulic valve dynamics, Energy 36 (2011) 6234–6242.
[16] J. Mao, Z. Zuo, D. Liu, Numerical simulation of a spark ignited two-stroke free piston engine generator, J. Beijing Inst. Technol. 18 (2009) 283–287.
[17] Q. Li, J. Xiao, Z. Huang, Simulation of a two-stroke free-piston engine for electrical power generation, Energy Fuel 22 (2008) 3443–3449.
[18] N. Hung, O. Lim, A study of a two-stroke free piston linear engine using numerical analysis, J. Mech. Sci. Technol. 28 (2014) 1545–1557.

[19] J. Xiao, Q. Li, Z. Huang, Motion characteristic of a free piston linear engine, Appl. Energy 87 (2010) 1288–1294.
[20] S. Xu, Y. Wang, T. Zhu, T. Xu, C. Tao, Numerical analysis of two-stroke free piston engine operating on HCCI combustion, Appl. Energy 88 (2011) 3712–3725.
[21] J. Fredriksson, I. Denbratt, Simulation of a Two-Stroke Free Piston Engine. SAE Technical Paper Series, 2004. 2004–01-1871.
[22] J. Mao, Z. Zuo, W. Li, H. Feng, Multi-dimensional scavenging analysis of a free-piston linear alternator based on numerical simulation, Appl. Energy 88 (2011) 1140–1152.
[23] H. Feng, C. Guo, C. Yuan, Y. Guo, Z. Zuo, A. Roskilly, et al., Research on combustion process of a free piston diesel linear generator, Appl. Energy 161 (2016) 395–403.
[24] Y. Miao, Z. Zuo, H. Feng, C. Guo, Y. Song, B. Jia, Y. Guo, Research on the combustion characteristics of a free-piston gasoline engine linear generator during the stable generating process, Energies 9 (2016) 655, https://doi.org/10.3390/en9080655.
[25] C. Yuan, H. Feng, Y. He, J. Xu, Motion characteristics and mechanisms of a resonance starting process in a free-piston diesel engine generator, Proc. Inst. Mech. Eng. Part A: J. Power Energy 230 (2016) 206–218.
[26] R. Mikalsen, A.P. Roskilly, A computational study of free-piston diesel engine combustion, Appl. Energy 86 (2009) 1136–1143.
[27] C. Zhang, F. Chen, L. Li, Z. Xu, L. Liu, G. Yang, H. Lian, Y. Tian, A free-piston linear generator control strategy for improving output power, Energies 11 (2018) 135–155.
[28] V. Shmelev, A. Margolin, Method of Conversion of Chemical Energy of a Fuel-air Mixture in Mechanical and Device for its Realization, Patent of RF 2138656, 1998.
[29] V. Shmelev, A. Margolin, Concern possibility of using poor mixtures in a free piston engine, Probl. Eng. Autom. 4 (1998) 65–69.
[30] J.I. Ramos, Internal Combustion Engine Modelling, HPB, New York, 1989.
[31] A. Hachiyan, K. Morozov, V. Lukanin, V. Trusov, D. Bagirov, E. Korsi, Internal Combustion Engines, Higher School, Moscow, 1985.
[32] V. Shmelev, V. Nikolaev, Partial oxidation of methane in a multistage-compression chemical reactor, Theor. Found. Chem. Eng. 42 (2008) 19–25.
[33] V. Shmelev, V. Nikolaev, Partial oxidation of methane in a rapid compression machine with internal heat recovery, Russ. J. Phys. Chem. B 2 (2008) 431–436.
[34] R. Petrenko, A Physical Base of Processes in ICE Cylinder, Leningrad University, Leningrad, 1983.
[35] K. Michenko, A. Ravdel (Eds.), Hand Book on Physical-chemical Data, Chemistry, Leningrad, 1972.
[36] V. Zamanckiy, A. Borisiv, The Totals of Science and Engineering, Kinetics and Catalysis, vol. 19, VINITI, Moscow, 1989.
[37] X. Hou, H. Zhanga, F. Yua, H. Liua, F. Yang, Y. Xuc, Y. Tian, G. Li, Free piston expander-linear generator used for organic Rankine cycle waste heat recovery system, Appl. Energy (2017), https://doi.org/10.1016/j.apenergy.2017.09.024.